Dyes and Pigments 142 (2017) 315–322

Contents lists available at ScienceDirect

Dyes and Pigments

journal homepage: www.elsevier.com/locate/dyepig

Room temperature phosphorescence lifetime and spectrum tuning of substituted thianthrenes

Piotr Pander [a, *], Agnieszka Swist [b], Jadwiga Soloducho [b], Fernando B. Dias [a]

[a] University of Durham, Department of Physics, South Road, Durham DH1 3LE, United Kingdom
[b] Wroclaw University of Technology, Faculty of Chemistry, Wybrzeze Wyspianskiego 27, 50-370 Wroclaw, Poland

ARTICLE INFO

Article history:
Received 13 January 2017
Received in revised form
22 March 2017
Accepted 23 March 2017
Available online 24 March 2017

Keywords:
RTP
RT-DFP
Phosphorescence
Thianthrene
Photophysics

ABSTRACT

A group of thianthrene derivatives has been studied to investigate the effect of different substituents and substitution positions on their photophysical behavior. Strong room temperature phosphorescence (RTP) and dual fluorescence-phosphorescence at room temperature (RT-DFP) have been observed. Compounds with efficient ($\Phi \approx 0.4$) yellow and long-lived ($\tau = 88 \pm 6$ ms) green phosphorescence have been characterized. The involvement of $n\pi^*$ and $\pi\pi^*$ states was evaluated to explain their high triplet formation yield and phosphorescent properties. To give an insight into electron properties of studied molecules cyclic voltammetry and DFT calculations have been performed.

1. Introduction

Thianthrene is a heterocyclic analog of anthracene but with two sulfur atoms substituting carbon atoms at the 9,10-positions. This structure leads to a bent, non-aromatic geometry of the central thianthrene ring [1–3]. Thianthrenes are commonly known due to their interesting electrochemical properties [3–7] and quite well studied chemistry [2,3,6,8]. Thianthrene being an electron-donor with a stable mono- and bicationic forms [4,7] has been used in several materials, including small molecules [2,6,8–11] and polymers [12,13]. Although the chemistry and electrochemistry of thianthrenes are well known, the photophysics has not been performed extensively. In particular, phosphorescent properties of thianthrene crystals have already been demonstrated [1], but no study has been performed on its derivatives. Of particular interest are the room temperature phosphorescent (RTP) properties of thianthrene, which suggests this group can be used to promote dual fluorescence-phosphorescence at room temperature in its derivatives, which brings additional interest on thianthrene based compounds. The aim of controlling and tuning luminescence of organic materials in the solid state is an attractive topic for both fundamental research, and for practical applications in several fields. For example, the observation of dual luminescence [14] e.g. dual fluorescence-phosphorescence emissions at room temperature, (RT-DFP), enhances the possibility to achieve tunable luminescent characteristics under external stimuli, which expands the potential of these compounds in photonic and optoelectronic applications.

Room temperature phosphorescence in purely organic, non-heavy-metal-containing molecules has been investigated for many years [1,15–23], and continues to be the topic of great interest, as confirmed by many recent publications, where RTP and RT-DFP are reported in several different systems [24–30]. Many of these molecules contain a non-metal *d*-electron element such as bromine, phosphorus, sulfur, tellurium or iodine, which enhances intersystem crossing from the emissive singlet state to the triplet state [15–23,31]. However, RTP or RT-DFP are observed usually in the crystalline [25] state, as powder, or in solid state blends, with the emitter dispersed in inert glassy host matrices made of amorphous polymers, such as PMMA, Zeonex® or in β-estradiol films that are non-permeable by oxygen [32]. Hosts are used to restrict the competitive thermal non-radiative decay pathways and facilitate the radiative decay of the triplet state. However, there are a few examples where surprisingly RTP has also been reported in solution [33].

While the strategies that have been implemented to restrict

* Corresponding author.
E-mail address: piotr.h.pander@durham.ac.uk (P. Pander).

http://dx.doi.org/10.1016/j.dyepig.2017.03.049

vibrations and induce RTP have gathered some success, further work is necessary to understand the mechanism driving RTP, and achieving design rules to obtain dual emitters is even a major challenge. It is still not clear why some emitters give origin to RT-DFP and others just to fluorescence, sometimes with very similar molecular structures and in the same host [34].

The main advantage of organic materials showing RT-DFP is the possibility to achieve ratiometric measurements due to the presence of fluorescence and phosphorescence bands that are observed simultaneously. This expands the dynamic range of the emission of these compounds and introduces an internal calibration, allowing their use in applications as optical thermometry [35–37], money anti-counterfeiting techniques [38], oxygen sensors [39], analytical chemistry [40], mechanochromic materials [30], and bioimaging [41], among others.

Optimization of RT-DFP emitters involves enhancing the total luminescence yield, and achieving a large separation of the fluorescent and phosphorescent bands, which expands the colorful emission switching under external stimuli. However, increasing the separation of the two emission bands, implies achieving a large energy gap between the singlet (S_1) and triplet (T_1) excited states which negatively impacts the triplet formation yield, due to less favorable intersystem crossing, and thus giving weaker phosphorescence yield [26]. Therefore RT-DFP molecules need to be designed in a way that the intersystem crossing is enhanced, while the singlet-triplet energy is tuned to give well separated emission bands. In this study we present a group of thianthrene derivatives (Scheme 1) examining the effect of both the substitution positions and the type of substituent on their room temperature phosphorescent properties. The aim of the study is to understand structural and electronic effects, such as produced steric hindrance or donor/acceptor properties, of popular substituents on thianthrene. We further examine the effect of $\pi\pi^*$ states on phosphorescence lifetime. Our results enabled us to understand the structure-property relationships in the RTP and RT-DFP systems based on thianthrene to further optimize the efficiency and performance of these emitters in future applications.

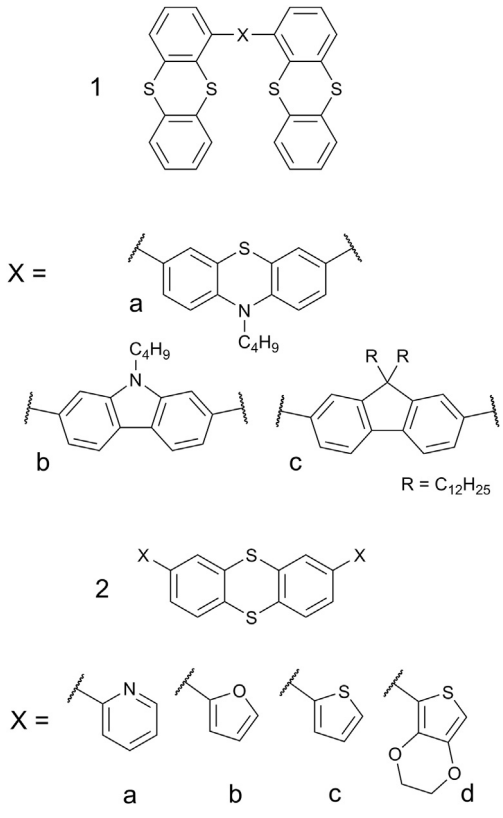

Scheme 1. A compendium of the thianthrene molecular structures studied in this work.

Interestingly, the phosphorescence in these thianthrenes, when dispersed in Zeonex® matrix, shows broad, featureless spectrum at room temperature. However, while compounds **1a** to **1c** are mainly RTP emitters, compounds **2a** to **2d** are dual emitters but with different fluorescence-phosphorescence ratios, with compound **2a** showing mainly phosphorescence, **2b** and **2c** showing dual fluorescence-phosphorescence bands, and **2d** showing mainly fluorescence. However, while **2b**, **2c** and **2d** have very low luminescence yields, **2a** is a strong emitter with the luminescence yield close to 40%. This is a significantly strong phosphorescence yield at RT for a metal-free pure organic emitter.

2. Materials and methods

2.1. Materials

Thianthrene derivatives were synthesized as described in previous work [3].

2.2. Photophysics

Absorption and fluorescence spectra were collected using a UV-3600 double beam spectrophotometer (Shimadzu), and a FluoroLog or FluoroMax-3 fluorescence spectrometer (Jobin Yvon). Low and room temperature measurements were acquired using a model liquid nitrogen cryostat (Janis Research) coupled with a rotary vacuum pump. Phosphorescence (PH) and prompt fluorescence (PF) spectra and decays were recorded using nanosecond gated luminescence and lifetime measurements (from 400 ps to 1 s) using a high energy pulsed Nd:YAG laser emitting at 355 (3rd harmonics) and 266 nm (4th harmonics) (EKSPLA). Emission was focused onto a spectrograph and detected on a sensitive gated iCCD camera (Stanford Computer Optics) having sub-nanosecond resolution. PF/PH time resolved measurements were performed by exponentially increasing gate and delay times. Photoluminescence quantum yield of solid films was done according to the procedure described elsewhere [42]. Blends of all materials in Zeonex® were made at 0.5–1% w/w concentration. Measurements taken at room temperature (295 ± 1 K) at all time unless stated otherwise. Fluorescence spectra in solution were recorded after degassing by 3 freeze/thaw cycles.

2.3. Electrochemistry

All measurements performed in 0.1 M Bu_4NBF_4 (99%, Sigma Aldrich) in dichloromethane (CHROMASOLV®, 99.9% Sigma Aldrich). Nitrogen bubbling was performed before measurement. Electrodes: working (Pt disc of 1 mm^2 area), counter (Pt wire), reference (Ag/AgCl calibrated against ferrocene). All cyclic voltammetry measurements conducted at room temperature with scan rate of 50 mV s^{-1}.

2.4. Calculations

DFT calculations of MO surfaces have been carried out using the B3LYP [43–45] hybrid functional combined with a 6-31G(d,p) [46–48] basis set. For all investigated compounds ground state geometries were optimized. All calculations have been carried out with Jaguar [49] version 9.1 in Maestro Materials Science 2.1 from

Maestro Materials Suite 2016-1 software package [50]. All alkyl chains have been reduced to methyl groups to decrease calculation complexity.

3. Results and discussion

3.1. Fluorescence and absorption spectra in solution and DFT calculations

The investigated materials were divided in two groups. The first one formed by compounds **1a**-**1c**, consists of molecules with two thianthrene moieties connected by a bridge, whereas the second group, compounds **2a**-**2d**, represents bisubstituted derivatives of thianthrene. All the compounds give blue fluorescence when dissolved in a non-polar solvent (Fig. 1). Interestingly, the emission spectrum within each group of materials is very similar. The fluorescence spectrum of **1a**-**1c** derivatives resembles thianthrene emission with the *onset* being only slightly red-shifted. Molecules **2a**, **2c** and **2d** show well-resolved fluorescence spectrum, but **2b** shows emission spectrum resembling thianthrene. Moreover, the fluorescence from compounds **2a**-**2d** appears clearly at lower energies than fluorescence of **1a**-**1c** as indicated by the *onset* of the fluorescence spectrum.

Before discussing the absorption spectra in Fig. 1, it is essential to note the key features of thianthrene absorption spectrum (Fig. 1). The reader can also refer to supporting information (Figs. S1 and S7). The UV-Vis spectrum of thianthrene in the presented wavelength range consists of two bands: 1) low energy band that forms a shoulder at $\lambda = 270–340$ nm with $\varepsilon < 3.5 \times 10^3$ $M^{-1}cm^{-1}$ which clearly indicates a forbidden transition such as an n-π^* transition involving the non-bonding electrons of sulfur; 2) the high energy band at $\lambda_{max} = 257$ nm with $\varepsilon \approx 4 \times 10^4$ $M^{-1}cm^{-1}$ that indicates a π-π^* transition.

In contrast, the absorption spectra of derivatives **1a**-**1c** consist of several absorption bands in the region of 270–360 nm where the thianthrene absorption is negligible. It is remarkable and interesting that the π-π^* absorption band of thianthrene $\lambda_{max} = 257$ nm can be clearly identified in **1a**-**1c** derivatives ($\lambda_{max} = 261–264$ nm, $\varepsilon \approx 0.4–1x10^5$ $M^{-1}cm^{-1}$). This is a strong indication that the thianthrene moiety in this case is not well conjugated with the bridge unit. The absorption of **1a** consists of a π-π^* absorption band at $\lambda_{max} = 314$ nm ($\varepsilon \approx 2 \times 10^4$ $M^{-1}cm^{-1}$) with a shoulder, presumably of a forbidden transition, most likely n-π^* of phenothiazine. There is also another band at $\lambda_{max} = 290$ nm. In **1b** the well-resolved band at 330–360 nm ($\varepsilon \approx 3–4x10^3$ $M^{-1}cm^{-1}$) is associated with n-π^* transition of carbazole. This is followed by an absorption band at $\lambda_{max} = 290$ nm. For **1c** the energetically lowest absorption band is clearly of π-π^* character $\lambda_{max} = 319$ nm ($\varepsilon \approx 7 \times 10^4$ $M^{-1}cm^{-1}$). This band is followed by absorption at $\lambda_{max} = 298$ nm.

Absorption spectra of **2a**-**2d** derivatives are very similar to each other. The absorption maximum ($\varepsilon \approx 3–4x10^4$ $M^{-1}cm^{-1}$) observed shifts gradually from **2a** ($\lambda_{max} = 277$ nm) through **2b** ($\lambda_{max} = 286$ nm) and **2c** ($\lambda_{max} = 287$ nm) to **2d** ($\lambda_{max} = 296$ nm). These absorption bands are associated with π-π^* transitions. It is worth to note that in this case the π-π^* absorption band of thianthrene is no longer observed. This might suggest that thianthrene is in this case a part of a larger conjugated system. A shoulder is also observed at 320–380 nm in the absorption spectra of molecules **2a**-**2d**, which is particularly evident in **2a**, and similar to pure thianthrene, this shoulder can be associated to a n-π^* transition. It is worth to note that overlap between those n-π^* and π-π^* absorption bands increases gradually from **2a** to **2d** which is expected to induce mixing of the nπ^* and $\pi\pi^*$ excited states thus formed.

The conclusions from the analysis of the UV-Vis spectra of the presented thianthrenes are consistent with the calculated HOMO and LUMO surfaces (Fig. 2 and Table S2). The thianthrene moiety shows a high contribution of non-bonding electrons of sulfur to the HOMO, which makes the HOMO → LUMO transition to be of n-π^* character. The same conclusion can be drawn from the observation of the HOMO in **2a**-**2d**, where the contribution of the non-bonding electrons of sulfur is particularly evident. In case of **1a**-**1c** the

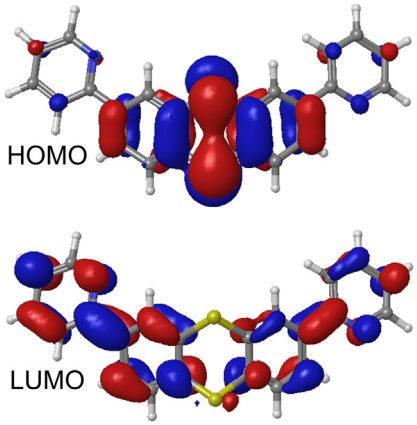

Fig. 2. Frontier molecular orbital surfaces at the B3LYP/6-31G(d,p) level for **2a**.

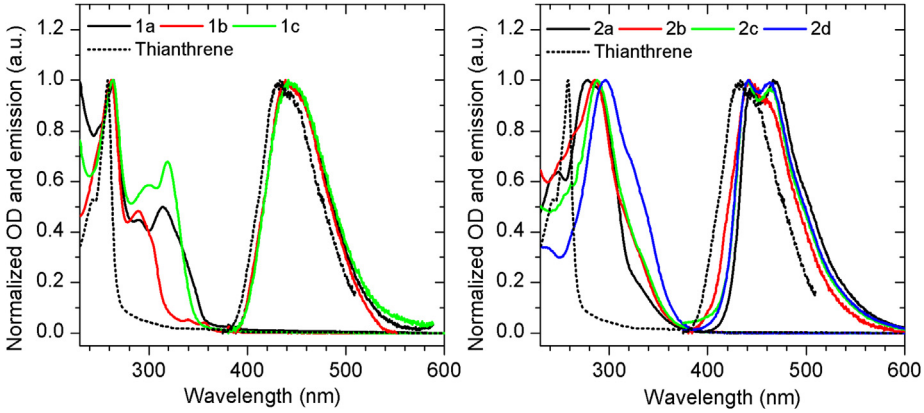

Fig. 1. Normalized photoluminescence and absorption spectra in methylcyclohexane (MCH). Recorded at room temperature. Fluorescence recorded in degassed solutions. $\lambda_{exc} = 330$ nm.

HOMO → LUMO transition is dominated by the bridge with some contribution of thianthrene to the LUMO. In **1a** the nitrogen and sulfur atoms of phenothiazine bridge clearly contribute to the HOMO with their non-bonding electrons, making the HOMO → LUMO transition to be n-π*. In **1b** the nitrogen atom of carbazole contributes to the HOMO giving somehow n-π* character to the energetically lowest transition. In **1c** the HOMO is clearly dominated by π-conjugated system of fluorene which indicates π-π* character of HOMO → LUMO transition.

3.2. Photoluminescence in solid state

All the molecules studied here show phosphorescence at room temperature that is comparable in intensity or much more intense than fluorescence (Fig. 3), when dispersed in a commercially available amorphous polymer Zeonex® 480 with high t_g = 138 °C [51] and noticeable air-permeability. The difference between emission recorded in air and in vacuum is due to the quenching of long-lived triplet states by oxygen. Therefore, by comparing the spectra in Fig. 3 in air and in vacuum it is possible to quantify the relative contributions of fluorescence and phosphorescence to the overall emission, with the assumption that in vacuum no triplet oxygen quenching effect is present. Fig. 3 also shows that in case of derivatives **1a**-**1c** and **2a** the contribution of phosphorescence is very high and exceeds 90% of the total photoluminescence at room temperature. This is more than for pure thianthrene. The high photoluminescent quantum yield in these compounds and the large contribution of phosphorescence to the total luminescence, see Table 1, indicates that the phosphorescence properties of thianthrenes **1a**-**1c** and **2a** are induced by a high triplet formation yield. This is caused by the presence of two sulfur atoms in the thianthrene core giving origin to an enhanced spin orbit coupling due to the presence of lone pairs in the sulfur and heavy atom effect. However, in the case of derivatives **2b**-**2d** the electron-donating effect (see below) of substituents causes reduction of the phosphorescence contribution to ≈50% in case of **2b** and **2c** and to only ≈25% in case of **2d**. In these compounds, the reduction in the phosphorescence contribution is accompanied by the observation of a weak fluorescence band at high energies. This indicates that in compounds **2b**-**2d** the radiative decay of the singlet excited state is able to compete with the slow intersystem crossing, and so less triplets are formed in these compounds (also see Table S1). Dual luminescence, i.e. RT-DFP, is thus achieved. However, the very low luminescence (fluorescence + phosphorescence) quantum yield of these compounds in solid state, roughly Φ < 0.1, without the presence of oxygen (Table 1) suggests that these thianthrenes are affected also by significant internal conversion.

The presented materials show strong dependance of emission intensity and photoluminescence color upon oxygen concentration. This is because the blue fluorescence is almost not affected by oxygen, while the phosphorescence is strongly suppressed by oxygen, therefore the fluorescence-phosphorescence ratio at a certain temperature is itself an indication of total amount of oxygen in the surrounding atmosphere.

3.3. Cyclic voltammetry

Cyclic voltammetry (CV) was chosen to investigate the first oxidation potential of thianthrenes to explain the effects of substituents on the electron-donating properties of the compounds. Withdrawal of the electron from the compound in a redox reaction is performed from its HOMO, therefore CV gives an insight into the properties of the highest occupied molecular orbital.

Oxidation of thianthrene is reversible (Fig. 4) as reported in the literature [5,7]. All presented thianthrenes, except **2d**, show reversible process as well. The oxidation *onset* potential of thianthrene 0.74 V is very close to the oxidation potentials of derivatives **1a**-**1c** and **2a**: 0.71–0.75 V. This behavior is especially surprising for **1a**, where electron-rich phenothiazine is expected to oxidize at lower potential (E_{ox} = 0.1 V vs. Fc/Fc^+) than thianthrene does [52].

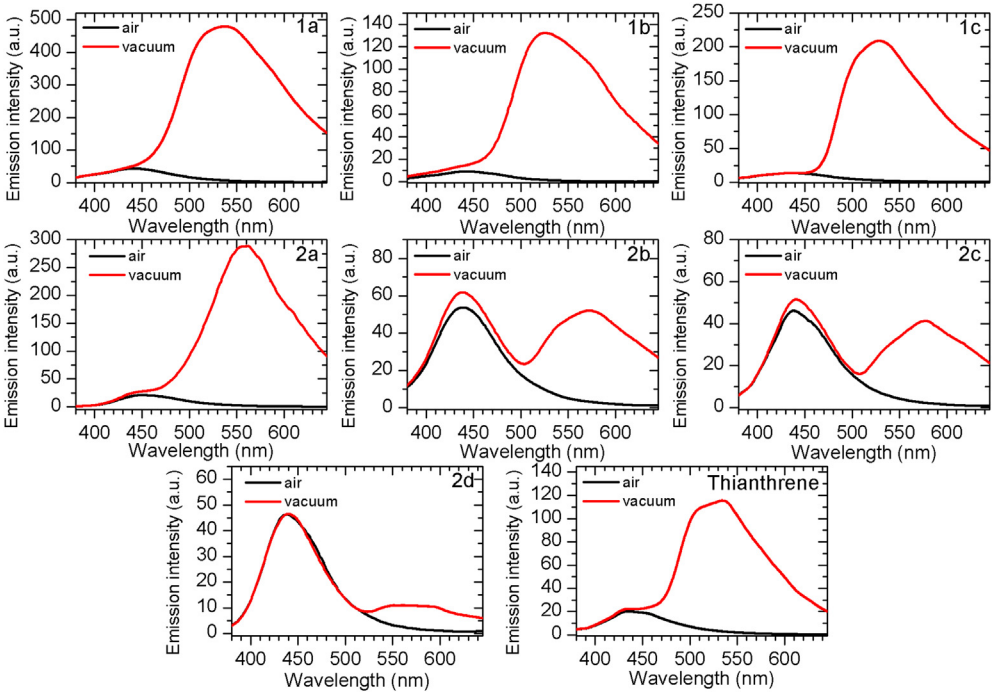

Fig. 3. Photoluminescence spectra in Zeonex® in presence of air and in vacuum. Recorded at 295 K using 330 nm excitation. Note the absorption spectra in Zeonex® can be found in Fig. S1.

Table 1
Spectroscopic and electrochemical data.

Compound	IP ± 0.02/EA ± 0.05, eV[a]	E_g^{op} ± 0.05, eV[b]	S_1/T_1 ± 0.05, eV[c]	τ_{PH}, ms[d]	Φ_{PL} ± 0.05[e]	%PH[f]
Thianthrene	5.84/–*	–*	3.13/2.70	18 ± 1	–	86
1a	5.85/2.37	3.48	3.09/2.71	18 ± 4 (54%) 2.9 ± 0.9 (46%) τ_{av} = 16**	0.15	93
1b	5.82/2.42	3.40	3.13/2.70	6.4 ± 0.3	0.22	94
1c	5.82/2.24	3.58	3.26/2.66	88 ± 6	0.12	94
2a	5.81/2.36	3.45	2.97/2.51	10.5 ± 0.5	0.42	94
2b	5.79/2.33	3.46	3.11/2.49	8.3 ± 0.6	0.04	50
2c	5.76/2.33	3.43	3.13/2.47	10.9 ± 0.4	0.06	49
2d	5.63/2.21	3.42	3.11/2.43	5.9 ± 0.2	0.04	24

*Due to the very weak absorption at the energetically lowest band shoulder, the optical energy gap cannot be estimated properly.
**Amplitude-weighted average lifetime.
[a] Ionization potential calculated from *onset* oxidation potential IP = E_{ox} + 5.1 [57–59]; Electron affinity estimated using equation EA = IP–E_g^{op}.
[b] Optical energy gap in toluene.
[c] Singlet and triplet energy at 295 K from prompt fluorescence and phosphorescence spectra in Zeonex®.
[d] Phosphorescence lifetime at 295 K in Zeonex®.
[e] Photoluminescence quantum yield in oxygen-free conditions in Zeonex® at room temperature, λ_{exc} = 330 nm.
[f] Percent contribution of phosphorescence in total photoluminescence at RT in oxygen-free conditions in Zeonex® matrix. HOMO and LUMO energy are commonly related to Ionization Potential (IP) and Electron Affinity (EA), respectively.

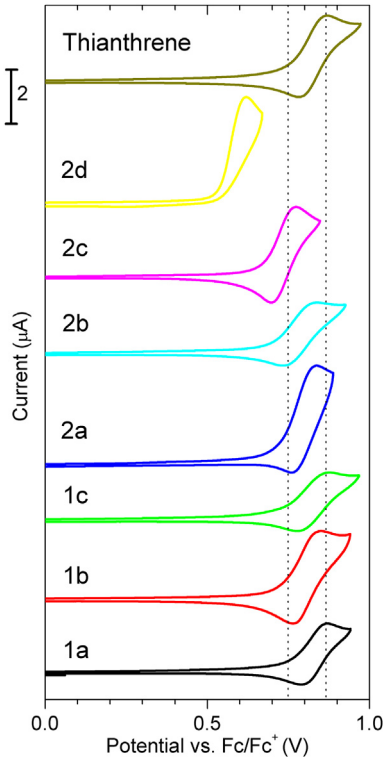

Fig. 4. Electrochemical oxidation of substituted thianthrenes in dichloromethane with 0.1 M Bu_4NBF_4 supporting electrolyte at 50 mV s^{-1} scan rate. The vertical dotted lines indicate *onset* and peak oxidation potential of thianthrene.

In case of derivatives **2a**-**2d** the oxidation potential lowers with the increase of electron-donating properties of substituent in the order from electron-deficient pyridine in **2a** to the most electron-rich ethylenedioxythiophene (EDOT) in **2d**. The electron-donating impact of the substituent in conjugated molecules **2b**-**2d** moves the HOMO towards the electron-rich groups (Table S2 in supporting information), therefore reducing the contribution of non-bonding electrons to the HOMO. In the most electron-rich **2d** the oxidation is centered mainly on the EDOT group which as a result gives an irreversible oxidation. EDOT and EDOT-containing molecules are known of being able to electropolymerize [53,54] and this is the most probable reason why **2d** shows irreversible oxidation. Film formation on the electrode has been observed as a consequence of electrooxidation of **2d** which confirms this statement.

Interestingly, the electrochemical oxidation of thianthrenes correlates with their photophysical behavior. In particular, the derivatives **1a**-**1c** and **2a** show large contribution of phosphorescence in total emission (>90%) (Table 1) – the same compounds for which the oxidation potential differs only ±0.04 V from the thianthrene. In case of **2b**-**2d** where the electron-donating effect of substituent starts to be important, the contribution of phosphorescence decreases dramatically to reach only ≈25% for **2d**. Moreover, with decreasing intensity of phosphorescence, structure of the **2d** spectrum is enhanced, which is particularly evident at low temperature.

3.4. Time-resolved photoluminescence study

Fig. 5 shows that the phosphorescence spectra of derivatives **1a**-**1c** at room temperature are almost identical to the phosphorescence spectrum of thianthrene under the same conditions, whereas derivatives **2a**-**2d** show a red-shifted spectrum. The difference between the 1 and 2-series of thianthrenes is the position where thianthrene is substituted. It was shown earlier in text that **2a**-**2d** compounds are well conjugated, whereas in **1a**-**1c**, due to steric hindrance, the conjugation between thianthrene and the bridge unit is broken. This is also consistent with MO surfaces and simulated molecular geometry (see Table S2).

It is also worth noting that the phosphorescence spectra of compounds **1a**-**1c** and **2a** are featureless, both at RT and 80 K, with the same effect being observed for pure thianthrene. However, low temperature spectra of **1a**, **1b** and **2a** are all blue-shifted in the same manner, with the exception of compound **1c**, for which the phosphorescence is not blue shifted. This shows that at higher temperatures the triplet state of these compounds is able to relax, probably due to the molecule adopting a new conformation and affecting the excited state of these thianthrenes derivatives. Remarkably, compounds **2b**-**2d** behave differently – their low temperature phosphorescence spectrum has a clear vibronic structure, and the *onset* of their phosphorescence spectrum does not shift with temperature, unlike that of **2a**, **1a**, and **1b**. The lack of structure in the phosphorescence spectrum, even at low temperature, can be a result of interconverting excited state conformers. Indeed, the thianthrene moiety is expected to wobble by the

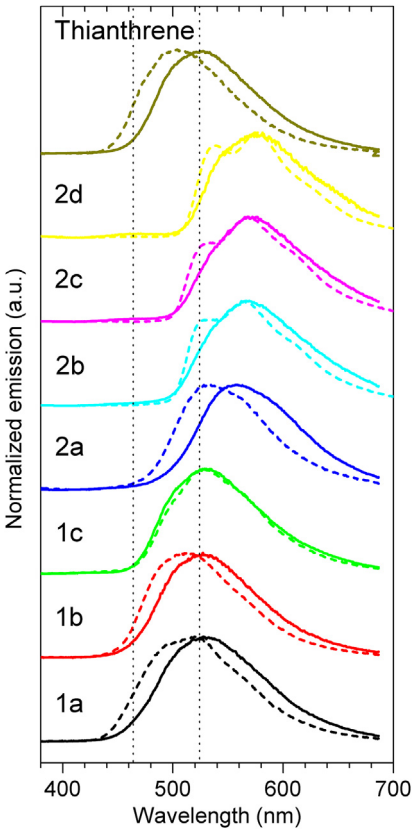

Fig. 5. Phosphorescence spectra recorded in Zeonex® at room temperature (solid line) and at 80 K (dashed line). Vertical dotted lines are an eye guide for *onset* and peak of thianthrene room temperature phosphorescence spectrum. Delay time >1 ms. λ_{exc} = 355 nm and 266 nm for thianthrene.

inversion of configuration at the sulfur atoms.

Moreover, in the **2a**-**2d** series the electron-donating/accepting properties of the substituents strongly affect the phosphorescence contribution to the overall luminescence and cause a significant effect on the phosphorescence spectrum. This suggests that the five-membered heterocyclic ring affects the electronic structure of thianthrene through conjugation and the effect escalates with electron-donating properties of the substituent (**2d**). In this case pyridine moieties in **2a**, that are acceptors, can be treated as the least electron-donating substituents. This is supported by the computational study (Table S3) that shows which in this series the dihedral angle between the substituent and respective thianthrene phenyl ring is small enough to allow conjugation. As a result of conjugation the electrochemical oxidation potential of derivatives **2a**-**2d** correlates with the results of the photophysical studies.

It is particularly clear that the behavior of **2a**-**2d**, is a consequence of their chemical structure and is closely related to their electronic structure which is expressed i.e. through electrochemical and calculation results. On the other hand, the mechanism causing the reduction in phosphorescence intensity in the series from **2a** to **2d** is related to an increase of both fluorescence and internal conversion rate constants.

Analysis of time-resolved emission spectra of **2a** reveals that a weak delayed fluorescence is also present (Fig. S5). However, power dependence studies, show that this delayed emission is due to triplet-triplet annihilation rather than thermally activated delayed fluorescence, moreover the singlet-triplet energy difference in **2a**, $\Delta E_{ST} = 0.46$ eV, is also too large for an efficient TADF to be observed.

Interestingly, the thianthrene molecules studied here, have comparable phosphorescence lifetimes of 6–16 ms, except **1c**, the fluorene derivative, which shows a lifetime around 88 ms. It is also significant that only **1c** shows lifetime of phosphorescence significantly different than pure thianthrene under the same conditions (18 ± 1 ms). The phosphorescence emission in this case is so long-lived that it can be observed by direct visual observation even a few seconds after laser excitation. This observation is fully consistent with the DFT calculations of MO surfaces, (Table S2), which show strong contribution of π electrons of fluorene to the HOMO whereas in all other molecules a non-bonding electron pair such as that of nitrogen or sulfur strongly contributes to the HOMO. At this point the HOMO → LUMO transition has the strongest π-π* character in compound **1c**, whereas in all the other cases it is mostly of n-π* character, which is also consistent with their UV-Vis absorption spectra (Fig. 1). In this case the fluorene moiety strongly affects not only the lowest singlet excited state, but also the lowest triplet state. This is particularly evident when the exceptional properties of **1c** phosphorescence are noted such as much longer lifetime or different behavior of the spectrum at RT and 80 K – no blue-shift at low temperature. This observation suggests the localization of the lowest triplet state on the fluorene moiety, whereas in other cases the T_1 properties are dominated or strongly affected by thianthrene. As the data suggest (Table S1) the fluorene moiety reduces the radiative rate constant of the triplet state, thus giving long-lived phosphorescence. This shows the potential to further improve the phosphorescence yield and increase the lifetime of thiantrene derivatives by suppression of the non-radiative decay.

Finally, all these thianthrenes derivatives show long phosphorescence lifetimes at room temperature, ranging from 6 to 88 ms (Fig. 6, Table 1). Moreover, the phosphorescence decays mono-exponentially in almost all cases, with exception of compound **1a**.

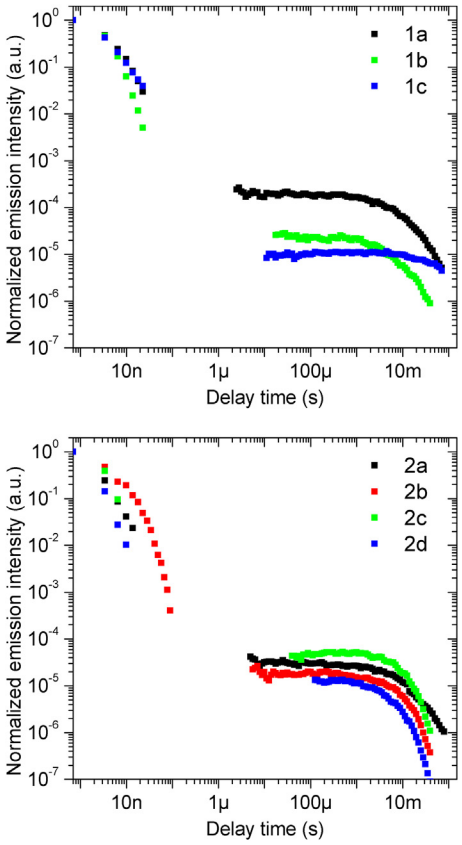

Fig. 6. Photoluminescence decays recorded in Zeonex® at room temperature, in vacuum. λ_{exc} = 355 nm and 266 nm for thianthrene.

The biexponential behavior of the phosphorescence decay in **1a** is accompanied by the change of the phosphorescence spectrum with time – a small blue-shift of the spectrum is observed at room temperature (Fig. S3). A similar, but less significant shift is observed in the case of compound **1c**, but this compound shows rather monoexponential decay. This behavior clearly suggests involvement of two emissive species in **1a** and **1c**. These species can either be two excited state conformers or two simultaneously emitting local triplet states. In the latter case the emissive states can be associated with thianthrene side groups and the bridge, whereas interconversion between the states is slow. In case of **1b** the carbazole has much higher triplet energy than thianthrene ($\approx$3 eV) [55,56] thus all energy is transferred to the lowest triplet state of thianthrene by internal conversion. This does not apply to **2a**-**2d** where the modifying group is conjugated with thianthrene resulting one excited state.

4. Conclusions

Thianthrene derivatives with different substituents and substitution positions have been shown as purely organic room temperature phosphorescent emitters with large (>90%) or moderate phosphorescence contribution to the total photoluminescence. Molecules showing green phosphorescence of lifetime $\tau = 88 \pm 6$ ms and strong ($\phi \approx 0.4$) yellow triplet emission have been presented. It has been shown that substituents of thianthrene may tune the lifetime of phosphorescence and fluorescence-phosphorescence ratio, thus giving a variety of RTP and DFP-RT emitters. On the other hand, tuning of the phosphorescence color is performed mainly by the extension of their conjugation. By substituting thianthrene at position 1- the substituents are weakly conjugated due to a steric hindrance – this results in green phosphorescence similar to that of thianthrene - whereas at 2,8- positions steric hindrance is reduced – conjugated systems show yellow triplet emission.

It has been observed that conjugated electron-rich substituents reduce the RTP intensity of thianthrene, they also have strong influence on the phosphorescence spectrum. This is due to depleting the n-π^* character of the excited state by conjugated π-donor furan/thiophene-based systems. Such a substituent reduces the triplet formation yield of molecule by inducing larger radiative and internal conversion rate constants of a singlet state. This phenomenon is well correlated with electrochemical *onset* oxidation potential and escalates with decrease of its value, so with increase in electron-donating effect of the substituent.

It has been presented that thianthrene may act as a RTP-promoting unit, which induces efficient intersystem crossing, whose phosphorescent properties may be tuned by substituents. Although thianthrene itself presents reasonable RTP properties, its absorption >280 nm is very weak which limits the possible application as an optical ratiometric sensor. Substitution of the thianthrene moiety with popular chromophores is therefore crucial to pave the way for possible applications due to introduction of strong π-π^* absorption bands in the region of 280–380 nm, which allows the molecules to be excited by popular light sources, such as nitrogen or Nd:YAG lasers and laboratory UV-lamps. This opens a new route of designing molecules for applications as room temperature phosphorescent agents. Numbers of possible modifications of thianthrene [2] show the possible pathways in future studies that also include their application as phosphorescent dyes with tunable phosphorescence color or metal-free OLED emitters.

Acknowledgments

Authors thank to Pawel Zassowski from Silesian University of Technology for fruitful discussions. Authors thank to EPSRC for funding this research by grant “The OLEDs without Iridium. 100% efficient triplet harvesting by Thermally Activated Delayed Fluorescence”, ref. EP/L02621X/1. The research leading to these results has received funding from the European Union's Horizon 2020 research and innovation programme under the Marie Skłodowska-Curie grant agreement No 674990 (EXCILIGHT). FBD thanks Samsung by funding this work using their Global Research Outreach (GRO) Program.

Appendix A. Supplementary data

Supplementary data related to this article can be found at http://dx.doi.org/10.1016/j.dyepig.2017.03.049.

References

[1] Arena A, Campagna S, Mezzasalma AM, Saija R, Saitta G. Analysis of the phosphorescence of thianthren crystals. Il Nuovo Cimento 1993;15(12):1521–32.
[2] Joule JJ. Thianthrenes. Adv Heterocycl Chem 1990;48:301–93.
[3] Swist A, Soloducho J, Data P, Lapkowski M. Thianthrene-based oligomers as hole transporting materials. Arkivoc 2012;(iii):193–209.
[4] Tinker LA, Bard AJ. Electrochemistry in liquid sulfur dioxide. 1. Oxidation of thianthrene, phenothiazine, and 9,10-diphenylanthracene. J Am Chem Soc 1979;101(9):2316–9.
[5] Janietz S, Wedel A. Electrochemical redox behavior and electroluminescence in the mixed energy-sufficient system thianthrene and 2- (4-biphenyl)-5-(4-*tert*-butylphenyl)-1,3,4-oxadiazole. Adv Mater 1997;9(5):403–7.
[6] Ogawa S, Muraoka H, Sato R. Design of reversible organic–organometallic multi-redox systems using thianthrene having ferrocene fragments. Tetrahedron Lett 2006;47:2479–83.
[7] Hammerich O, Parker VD. The reversible oxidation of aromatic cation radicals to dications. Solvents of low nucleophilicity. Electrochim Acta 1973;18:537–41.
[8] Lovell JM, Beddoes RL, Joule JA. Synthesis of 4,6-disubstituted thianthrenes; X-ray crystal structures of 4,6-diphenylthianthrene and 1-tetrathiafulvalenylnaphthalene. Tetrahedron 1996;52(13):4745–56.
[9] Sato K, Hyodo M, Aoki M, Zheng X-Q, Noyori R. Oxidation of sulfides to sulfoxides and sulfones with 30% hydrogen peroxide under organic solvent- and halogen-free conditions. Tetrahedron 2001;57:2469–76.
[10] Sun K, Jiang W, Ban X, Huang B, Zhang Z, Ye M, et al. Novel aggregation-induced emission and thermally activated delayed fluorescence materials based on thianthrene-9,9',10,10'-tetraoxide derivatives. RSC Adv 2016;6:22137–43.
[11] Wroblowska M, Kudelko A, Kuznik N, Laba K, Lapkowski M. Synthesis of extended 1,3,4-oxadiazole and 1,3,4-thiadiazole derivatives in the suzuki cross-coupling reactions. J Heterocycl Chem 2016. http://dx.doi.org/10.1002/jhet.2743.
[12] You N-H, Chueh C-C, Liu C-L, Ueda M, Chen W-C. Synthesis and memory device characteristics of new sulfur donor containing polyimides. Macromolecules 2009;42:4456–63.
[13] Johnson RA, Mathias LJ. Thianthrene-containing polymers: polyimides, aramids, and polybenzoxazoles in step-growth polymers for high-performance materials. ACS Symp Ser 1996;624:403–20 [chapter 26].
[14] Reineke S, Seidler N, Yost SR, Prins F, Tisdale WA, Baldo MA. Highly efficient, dual state emission from an organic semiconductor. Appl Phys Lett 2013;103:093302.
[15] Mukherjee S, Thilagar P. Recent advances in purely organic phosphorescent materials. Chem Commun 2015;51:10988–1003.
[16] Kitade T, Kitamura K, Kishimoto N. Determination of some phenothiazine derivatives by room-temperature phosphorimetry on a poly(vinyl alcohol) substrate. Anal Sci 1996;12:439–41.
[17] Gifford LA, Miller JN, Phillipps DL, Thorburn Burns D, Bridges JW. Phosphorimetric analysis of phenothiazine derivatives. Anal Chem 1975;47(9):1699–702.
[18] Canabate Diaz B, Schulman SG, Segura Carretero A, Fernandez Gutierrez A. Study of the substituent groups effect on the room-temperature phosphorescent emission of fluorene derivatives in solution. Anal Chim Acta 2003;489:165–71.
[19] Hurtubise RJ, Thompson AL, Hubbard SE. Solid-phase room-temperature phosphorescence. Anal Lett 2005;38:1823–45.
[20] Bruzzone L, Badia R. Room-temperature phosphorescence of impure fluorene. Anal Lett 1990;23(6):1113–21.
[21] Peng YL, Wang YT, Wang Y, Jin WJ. Current state of the art in cyclodextrin-induced room temperature phosphorescence in the presence of oxygen. J Photochem Photobiol A 2005;173:301–8.
[22] Liu, Y.; Zhan, G.; Liu, Z.-W.; Bian, Z.-Q.; Huang, C.-H. Room-temperature phosphorescence from purely organic materials. Chin Chem Lett. http://doi.org.10.1016/j.cclet.2016.06.029.

[23] Zhang G, Chen J, Payne SJ, Kooi SE, Demas JN, Fraser CL. Multi-emissive difluoroboron dibenzoylmethane polylactide exhibiting intense fluorescence and oxygen-sensitive room-temperature phosphorescence. J Am Chem Soc 2007;129:8942–3.
[24] Bolton O, Lee K, Kim H-J, Lin KY, Kim J. Activating efficient phosphorescence from purely organic materials by crystal design. Nat Chem 2011;3:205–10.
[25] An Z, Zheng C, Tao Y, Chen R, Shi H, Chen T, et al. Stabilizing triplet excited states for ultralong organic phosphorescence. Nat Mater 2015;14:685–90.
[26] Mao Z, Yang Z, Mu Y, Zhang Y, Wang Y-F, Chi Z, et al. Linearly tunable emission colors obtained from a fluorescent–phosphorescent dual-emission compound by mechanical stimuli. Angew Chem Int Ed 2015;54:6270–3.
[27] Hirata S, Totani K, Kaji H, Vacha M, Watanabe T, Adachi C. Reversible thermal recording media using time-dependent persistent room temperature phosphorescence. Adv Opt Mater 2013;1:438–42.
[28] Reineke S, Seidler N, Yost SR, Prins F, Tisdale WA, Baldo MA. Highly efficient, dual state emission from an organic semiconductor. Appl Phys Lett 2013;103:093302.
[29] Yang Z, Mao Z, Zhang X, Ou D, Mu Y, Zhang Y, et al. Intermolecular electronic coupling of organic units for efficient persistent room-temperature phosphorescence. Angew Chem Int Ed 2016;55:2181–5.
[30] Gong Y, Chen G, Peng Q, Yuan WZ, Xie Y, Li S, et al. Achieving persistent room temperature phosphorescence and remarkable mechanochromism from pure organic luminogens. Adv Mater 2015;27:6195–201.
[31] He G, Delgado WT, Schatz DJ, Merten C, Mohammadpour A, Mayr L, et al. Coaxing solid-state phosphorescence from tellurophenes. Angew Chem Int Ed 2014;53:4587–91.
[32] Hirata S, Totani K, Zhang J, Yamashita T, Kaji H, Marder SR, et al. Efficient persistent room temperature phosphorescence in organic amorphous materials under ambient conditions. Adv Funct Mater 2013;23:3386–97.
[33] Xu J, Takai A, Kobayashi Y, Takeuchi M. Phosphorescence from a pure organic fluorine derivative in solution at room temperature. Chem Commun 2013;49:8447–9.
[34] Dias FB, Bourdakos KN, Jankus V, Moss KC, Kamtekar KT, Bhalla V, et al. Triplet harvesting with 100% efficiency by way of thermally activated delayed fluorescence in charge transfer OLED emitters. Adv Mater 2013;25:3707–14.
[35] Kucsko G, Maurer PC, Yao NY, Kubo M, Noh HJ, Lo PK, et al. Nanometre-scale thermometry in a living cell. Nature 2013;500:54–8.
[36] Jethi L, Krause MM, Kambhampati P. Toward ratiometric nanothermometry via intrinsic dual emission from semiconductor nanocrystals. J Phys Chem Lett 2015;6:718–21.
[37] Jaque D, Vetrone F. Luminescence nanothermometry. Nanoscale 2012;4:4301–26.
[38] Jiang K, Zhang L, Lu J, Xu C, Cai C, Lin H. Triple-mode emission of carbon dots: applications for advanced anti-counterfeiting. Angew Chem Int Ed 2016;55:7231–5.
[39] Sanchez-Barragan I, Costa-Fernandez JM, Valledor M, Campo JC, Sanz-Medel A. Room-temperature phosphorescence (RTP) for optical sensing. Trends Anal Chem 2006;25(10):958–67.
[40] Kuijt J, Ariese F, Brinkman UAT, Gooijer C. Room temperature phosphorescence in the liquid state as a tool in analytical chemistry. Anal Chim Acta 2003;488:135–71.
[41] Zhang G, Palmer GM, Dewhirst MW, Fraser CL. A dual-emissive-materials design concept enables tumour hypoxia imaging. Nat Mater 2009;8(9):747–51.
[42] De Mello JC, Wittmann HF, Friend RH. An improved experimental determination of external photoluminescence quantum efficiency. Adv Mater 1997;9:230–2.
[43] Becke AD. A new mixing of Hartree-Fock and local density-functional theories. J Chem Phys 1993;98:1372–7.
[44] Becke AD. Density-functional thermochemistry. III. The role of exact exchange. J Chem Phys 1993;98:5648–52.
[45] Lee C, Yang W, Parr RG. Development of the colle-salvetti correlation-energy formula into a functional of the electron density. Phys Rev B 1988;37:785–9.
[46] Rassolov VA, Ratner MA, Pople JA, Redfern PC, Curtiss LA. 6-31G* basis set for third-row atoms. J Comp Chem 2001;22:976–84.
[47] Rassolov VA, Pople JA, Ratner MA, Windus TL. 6-31G* basis set for atoms K through Zn. J Chem Phys 1998;109:1223–9.
[48] Blaudeau J-P, McGrath MP, Curtiss LA, Radom L. Extension of Gaussian-2 (G2) theory to molecules containing third-row atoms K and Ca. J Chem Phys 1997;107:5016–21.
[49] Bochevarov AD, Harder E, Hughes TF, Greenwood JR, Braden DA, Philipp DM, et al. Jaguar: a high-performance quantum chemistry software Program with strengths in life and materials sciences. Int J Quantum Chem 2013;113(18):2110–42.
[50] Materials science suite 2016-1. Schrödinger. LLC, New York, NY, 2016.
[51] http://www.zeon.co.jp/content/200181690.pdf [Accessed 19 November 2016].
[52] Nobuyasu RS, Ren Z, Griffiths GC, Batsanov AS, Data P, Yan S, et al. Rational design of TADF polymers using a DA monomer with enhanced TADF efficiency induced by the energy alignment of charge transfer and local triplet excited states. Adv Opt Mater 2016;4:597–607.
[53] Zykwinska A, Domagala W, Lapkowski M. ESR spectroelectrochemistry of poly(3,4-ethylenedioxythiophene) (PEDOT). Electrochem Commun 2003;5:603–8.
[54] Data P, Zassowski P, Lapkowski M, Domagala W, Krompiec S, Flak T, et al. Electrochemical and spectroelectrochemical comparison of alternated monomers and their copolymers based on carbazole and thiophene derivatives. Electrochim Acta 2014;122:118–29.
[55] Castex MC, Olivero C, Pichler G, Ades D, Siove A. Fluorescence, room temperature phosphorescence and photodegradation of carbazole compounds in irradiated poly(methyl methacrylate) matrices. Synth Met 2006;156:699–704.
[56] Hoffmann ST, Schrogel P, Rothmann M, Albuquerque RQ, Strohriegl P, Kohler A. Triplet excimer emission in a series of 4,4′-Bis(N-carbazolyl)-2,2′-biphenyl derivatives. J Phys Chem B 2011;115(3):414–21.
[57] Cardona CM, Li W, Kaifer AE, Stockdale D, Bazan GC. Electrochemical considerations for determining absolute frontier orbital energy levels of conjugated polymers for solar cell applications. Adv Mater 2011;23:2367–71.
[58] Data P, Pander P, Lapkowski M, Swist A, Soloducho J, Reghu RR, et al. Unusual properties of electropolymerized 2,7- and 3,6- carbazole derivatives. Electrochim Acta 2014;128:430–8.
[59] Bredas J-L. Mind the gap! Mater Horiz 2014;1:17–9.